REMOTE SENSING LETTERS
2019, VOL. 10, NO. 12, 1192–1200
https://doi.org/10.1080/2150704X.2019.1671634

Taylor & Francis
Taylor & Francis Group

Use of spatial autocorrelation and time series Landsat images for long-term monitoring of surface water shrinkage and expansion in Guanting Reservoir, China

Zhichao Li[a], Yujie Feng[b], Helen Gurgel[c], Lei Xu[a], Nadine Dessay[d] and Peng Gong[a,e]

[a]Ministry of Education Key Laboratory for Earth System Modeling, Department of Earth System Science, Tsinghua University, Beijing, China; [b]School of Software and Microelectronics, Peking University, Beijing, China; [c]Department of Geography, University of Brasilia, Brasilia, Brazil; [d]ESPACE-DEV, UMR 228 IRD/UM/UR/UG, Institut de Recherche pour le Développement, Montpellier, France; [e]Joint Center for Global Change Studies, Beijing, China

ABSTRACT

Reservoirs are closely related to anthropic activities, and quantifying the long-term dynamics of surface water in reservoirs could be useful for decision-makers to improve the actual strategies of reservoir management. This study used the global Moran's I index, modified Normalized Difference Water Index (MNDWI) and a total of 596 Landsat images during 1985–2018 for tracking the annual dynamics of water extent in the process of water shrinkage and expansion in Guanting Reservoir, China. Landscape metrics related to the area, elongation, fragmentation, and edge complexity of surface water in reservoir landscape were computed for tracking the annual dynamics of surface water patterns. Statistical comparison between the results of global Moran's I index and landscape metrics indicates that except for the complexity of water and non-water edge, global Moran's I index can successfully estimate the dynamics of the area, elongation and fragmentation of surface water in the reservoir. This study proposed a continuous approach of long-term monitoring of surface water patterns using spatial autocorrelation that might be used in the areas where the surface water extraction is difficult and water dynamics are complex.

ARTICLE HISTORY
Received 15 July 2019
Accepted 12 September 2019

1. Introduction

Reservoirs are often formed for supporting anthropic activities, such as freshwater supply, agriculture irrigation and hydropower production, and their construction offers an obvious increase in the number, area and spatial distribution of surface water in many regions of the world (Drakou et al. 2008; Havel, Lee, and Zanden 2005). Quantifying the dynamics of surface water are fundamental in the hydrological, biogeochemical and ecological studies that were useful for decision-makers to improve the strategies of reservoir management (Wang et al. 2019).

CONTACT Peng Gong penggong@mail.tsinghua.edu.cn Ministry of Education Key Laboratory for Earth System Modeling, Department of Earth System Science, Tsinghua University, Beijing, China

Optical remote sensing data were widely applied for tracking the dynamics of surface water in recent years, such as SPOT 5 (Fisher and Danaher 2013), Sentinel-2 data (Yang et al. 2017), Landsat 5 Thematic Mapper (TM), Landsat 7 Enhanced Thematic Mapper Plus (ETM+) and Landsat 8 Operational Land Imager (OLI) data (Li et al. 2019; Zou et al. 2018) and Moderate Resolution Imaging Spectroradiometer (MODIS) data (Ji et al. 2018; Feng et al. 2012). Considering the spatial and temporal resolution, and time span of these data, time series Landsat images are the compromise solution that permits a long-term tracking (Pflugmacher 2007) of the dynamics of surface water, especially using all available Landsat images covering the same study area (Xu 2018). In term of water extraction algorithms, many studies used multi-spectral indices (e.g. modified Normalized Difference Water Index (MNDWI)) as they are quite easy and quick for computation (Li et al. 2019; Xu 2018; Zou et al. 2018). Then, thresholding methods are needed for extracting the surface water from the results of multi-spectral indices. Otsu's method (Otsu 1979), one of the most common methods, permits to automatically give the real time threshold values by maximizing the inter-class variance of surface water and background features, and therefore adapts well to the spectral index with a bi-model distribution (Du et al. 2014, 2016). It is able to respect the different study areas, weather conditions and time of satellite image acquisition (Li et al. 2015, 2019; Du et al. 2014). Researchers often used landscape metrics for quantifying the compositional and configurational patterns of land use and land cover (LULC) types and their changes in a landscape, particularly the dynamics of the surface water patterns in wetlands landscape (Li et al. 2019; Jiang et al. 2014; Zhao et al. 2008; Evans, Robinson, and Rooney 2017). Besides, spatial autocorrelation, such as global Moran's I index, was often used for describing the data clustering patterns, which is also able to indicate the changes of the clustering patterns of land cover types (Das and Ghosh 2017). Such a method might be another option for investigating the dynamics of surface water patterns.

As one of the lake-type reservoirs, Guanting Reservoir has been the important water source for anthropic activities in municipal sectors of Beijing, the capital of China where the evident dynamics of surface water shrinkage and expansion based on water area over the past three decades have been observed (Wang et al. 2019). However, the long-term dynamics of the surface water patterns in reservoir landscape have not yet been studied. In this context, this study aims to investigate whether global Moran's I index can give an overall retrospect of the dynamics of surface water patterns in the process of water shrinkage and expansion in Guanting Reservoir during 1985–2018, by comparing its performance with landscape metrics.

2. Study area

This study was carried out in Guanting Reservoir that is located northwest of Beijing, the capital of China (Figure 1). During the past three decades, it presented an obvious alternation of surface water shrinkage and expansion, with the four following stages: i) slow rising during 1985–1995, ii) severe atrophy during 1996–2007, iii) stable status during 2008–2012, and iv) recovery during 2013–2016 (Wang et al. 2019). Meanwhile, Guanting Reservoir suffered from the extensive problems of water quality due to the nutrients and organic carbon loading from the drainage catchments (Yihui, Guihuan, and Rui 2018; He et al. 2011; Liu et al. 2015). The national and municipal water-related

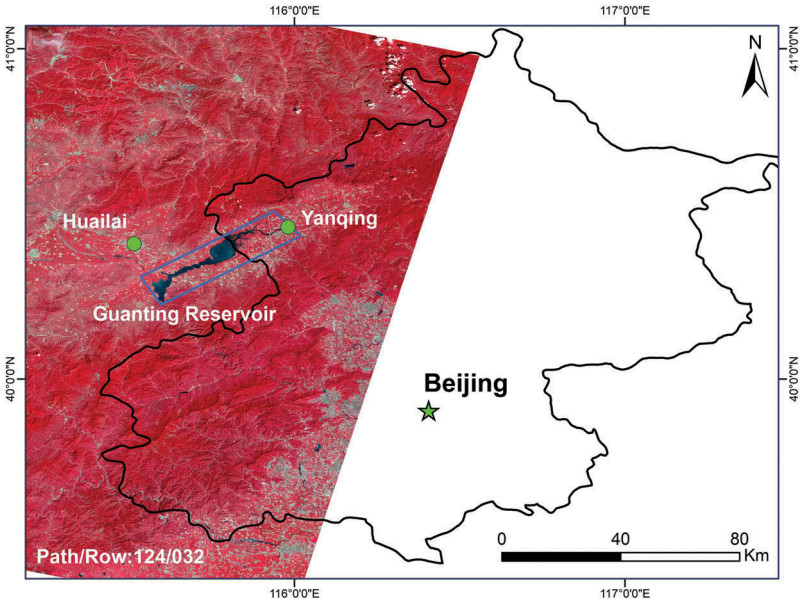

Figure 1. Geographic location of Guanting Reservoir. The blue block represents the area where all the statistical analysis were realized in this study. They were displayed on the Landsat 8 OLI (date: 21-08-2018) false-colour composite image using the Green, Red and NIR bands.

policies have been implemented for resolving the problems of water quality and water storage in the past years that not only alleviated the water pollution, but also evidently affected the dynamics of water extent (Wang et al. 2019).

3. Materials and methods

3.1. Yearly MNDWI composites

All available Landsat surface reflectance data derived from the Landsat 5 TM, Landsat 7 ETM+ and Landsat 8 OLI over the period 1985–2018 were collected from the United States Geological Survey (USGS) website and were used as the input data for computing spectral index (Figure 2(a)). All Landsat images have been pre-processed to L1TP level (i.e., Standard Terrain Correction) or L1GT level (i.e., Systematic Terrain Correction). For each image, a quality assessment band was used to remove cloud and cloud shadow, and the vector file of the bleu block (Figure 1) was applied to delineate the study area. Then, MNDWI was applied to each observation from 1985 to 2018 for producing the MNDWI time series.

$$MNDWI = \frac{\text{Green} - SWIR1}{\text{Green} + SWIR1} \tag{1}$$

where *Green* and *SWIR1* represent the surface reflectance value of the green band (band 2 for Landsat TM/ETM+ data and band 3 for Landsat OLI data) and shortwave infrared band (band 5 for Landsat TM/ETM+ data and band 6 for Landsat OLI data), respectively.

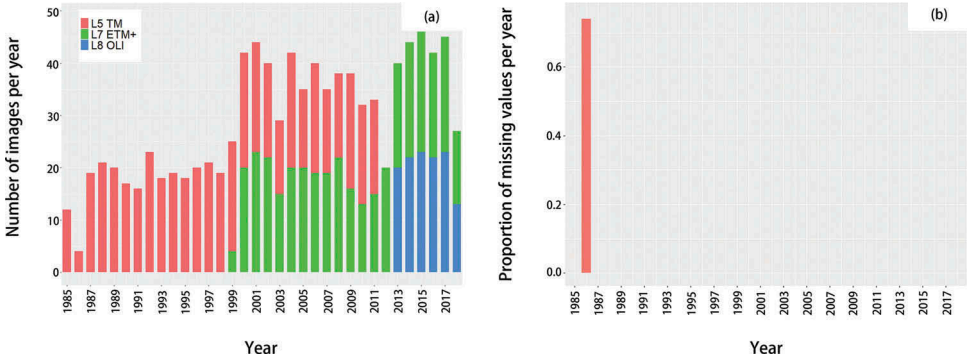

Figure 2. Landsat data availability covering the study area during 1985–2018. (a) Number of Landsat 5, 7 and 8 images per year; (b) Number of missing values per study period of each year (i.e., from April to October).

Based on a mean reducer (Sun et al. 2019), the MNDWI layers between April and October of each year were utilized to generate the yearly MNDWI composite, as the ice might be present on the water surface from November to March that could affect the values of MNDWI. Figure 2b shows the histogram of the proportion of missing values in each yearly MNDWI composite covering the study area, and the yearly MNDWI composite for 1986 was not included in the computation of spatial autocorrelation index and landscape metrics due to the presence of missing values.

3.2. Spatial autocorrelation index

Global Moran's I (Cliff and Ord 1981) is a widely used spatial autocorrelation index, was applied on yearly MNDWI composites for measuring the dynamics of surface water patterns. The index values varied from 1 to −1, and the value 1 means the positive spatial autocorrelation (i.e., cluster patterns), the value −1 means the negative spatial autocorrelation (i.e., chequerboard patterns), and the value 0 represents no autocorrelation (i.e., random patterns). In this study, based on the queen's case of spatial contiguity, global Moran's I was estimated using the *Moran* function in the package *raster* in R, and we obtained one value of spatial autocorrelation per year during the entire study period. The global Moran's I (I) could be expressed as follows:

$$I = \frac{n\sum_{i=1}^{n}\sum_{j=1}^{n} w_{ij}(x_i-\bar{x})(x_j-\bar{x})}{\left(\sum_{i=1}^{n}\sum_{j=1}^{n} w_{ij}\right)\sum_{i=1}^{n}(x_i-\bar{x})^2}(i\neq j) \tag{2}$$

where n is the number of locations in the each of yearly MNDWI composites, x_i and x_j represent the values of MNDWI at locations i and j, respectively. $\bar{x}$ is the average value of MNDWI in all locations, and w_{ij} represents the spatial proximity between locations i and j.

3.3. Landscape metrics

Considering the shrinkage and expansion of surface water in reservoir landscape, the compositional feature of surface water was characterized by the percentage (PLAND) of water, and the configurational patterns of surface water were characterized by area-weighted mean-related circumscribing circle (CIRCLE_AM), edge density (ED), and landscape division index (DIVISION) that permit to describe the elongation, fragmentation, and complexity of water *vs*. non-water landscape, respectively (Table 1). Based on yearly MNDWI composites, we first used Otsu's method for separating water and non-water, and generating the yearly water *vs*. non-water maps. Then, based on yearly water *vs*. non-water maps, landscape metrics were computed with an 8-connectivity implementation of the algorithm, using Fragstats software 4.2 (Amherst, MA, USA).

3.4. Statistical and comparative analysis

In order to evaluate the performance of global Moran's I in the description of the dynamics of surface water patterns, we first normalized both landscape metrics and global Moran's I of MNDWI using min-max method for ensuring their values varying from 0 to 1. Such method has been applied in the quantitative comparison of diverse landscape metrics (Li et al. 2016). Then, the statistical relationships between landscape metrics and global Moran's I of MNDWI were established using second-degree polynomial regression and coefficient of determination (R^2).

4. Results and discussion

4.1. Relationship between global moran's i of MNDWI and landscape metrics

Figure 3 presents the variation of global Moran's I of MNDWI and the percent of water obtained from class-level metric PLAND during the entire study period. It is evident that all the values of global Moran's I were near to 1. This indicates that surface water in Guanting Reservoir kept the cluster patterns during the entire study period. However, a graphical trend could be clearly observed. The values of global Moran's I of MNDWI had a relatively stable status from 1985 to 1995, and it severely decreased from 1996 to 2012, followed by a sharp increase from 2012. The overall variation of global Moran's I of MNDWI was similar with the trend of per cent of water (Figure 3) and the process of water extent dynamic proposed by (Wang et al. 2019).

Figure 4 illustrates the variations in landscape metrics as a function of the global Moran's I of MNDWI. The global Moran's I of MNDWI exhibited very significant (p-value <0.001) relationship with PLAND, CIRCLE_AM and DIVISION, with the coefficient of determination equal to 0.79, 0.85 and 0.79, respectively. These results could explain that global Moran's I of MNDWI was sensitive with the changes in the area, elongation and fragmentation of surface water in reservoir landscape. However, ED did not have a significant relationship with global Moran's I of MNDWI. It means that global Moran's I index cannot represents the edge complexity of the water and non-water landscape.

Table 1. Landscape metrics used in this study.

Metric (Abbreviation)	Description	Units	Range
Percentage (**PLAND**)	Proportional abundance of water patches in study area	%	(0, 100)
Edge density (**ED**)	Total length of patch edges in study area, per hectare	m ha^{-1}	≥0
Area-weighted mean related circumscribing circle (**CIRCLE_AM**)	Assessing shape based on the ratio of patch area to the area of the smallest circumscribing circle, for each patch in study area.	No unit	(0, 1)
Landscape division index (**DIVISION**)	Probability that two randomly chosen pixels in study area are not situated in the same patch	Proposition	(0, 1)

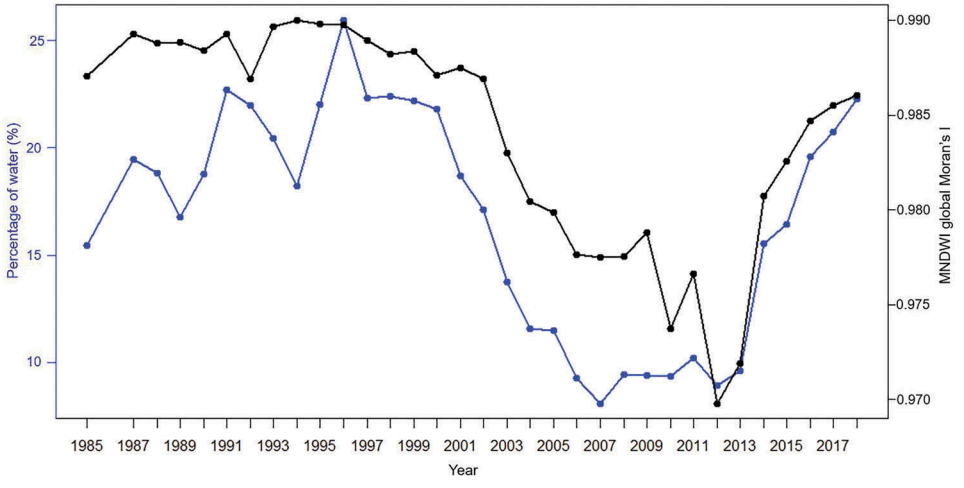

Figure 3. Temporal variation of the percentage of water (blue line) and the values of MNDWI global Moran's I (black line) during 1985–2018.

The reliability of the results could be explained by the clear separation between water and non-water in each yearly MNDWI composite histogram, with the values corresponding to water class varied from 0.3 to 0.8, and the values corresponding non-water class varied from −0.5 to −0.2. In fact, surface water has a high reflectance in green wavelength and virtually no reflectance in the shortwave infrared wavelength. Moreover, there are very few pixels that might affect the surface water extraction, such as pixels of terrain shadows and cloud shadows in each yearly MNDWI composite as the terrain of the study area is relatively flat, and clouds and cloud shadows were removed. These facts can ensure: (i) the effective and accurate monitoring of water extent shrinkage and expansion patterns using global Moran's I of yearly MNDWI composites, as this spatial autocorrelation index uses not only the information on spatial arrangement of pixels in input raster but also pixel values; (ii) the easy and accurate separation of water and non-water from the yearly MNDWI composites using Otsu's algorithm, which then ensures the ability of landscape metrics reflecting the real situation of surface water dynamics in Guanting Reservoir.

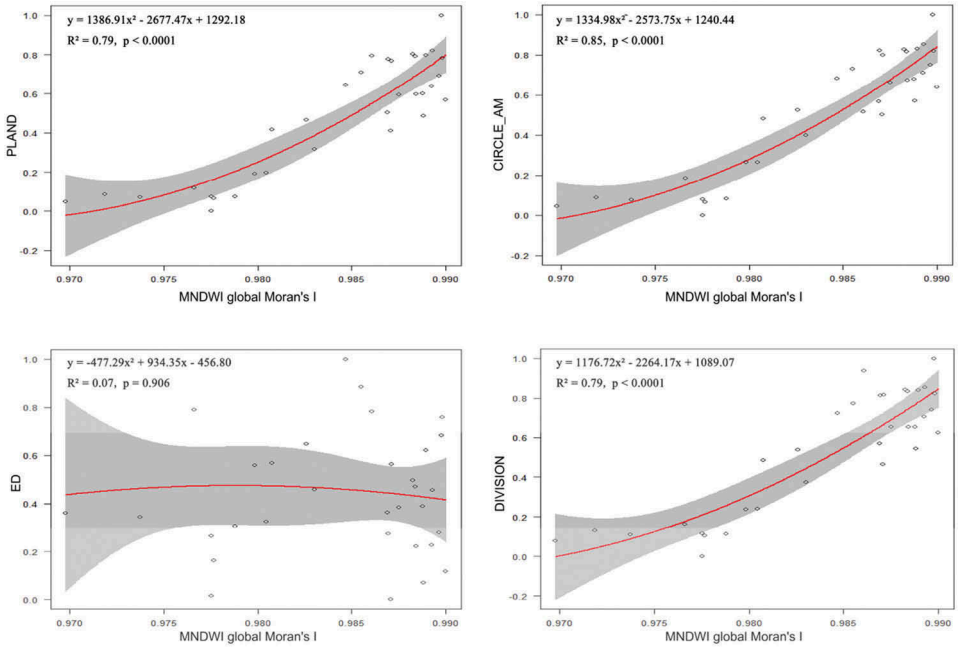

Figure 4. Comparison between the results of MNDWI global Moran's I and landscape metrics. The red line represents the regression line obtained using a second-degree polynomial regression.

4.2. Limitations and further considerations

This study has certain limitations. First, we solely considered the global Moran's I index in this study, other spatial autocorrelation indices should be considered in further studies. Second, significant results were obtained in Guanting Reservoir that is an artificial reservoir with evident water extent dynamics and relatively simple land surface. Further studies could apply the proposed framework in the natural wetlands for validating its performance where both dynamic of surface water patterns and landscape are often complex and diverse. Third, due to the small size of study area, it cannot prove the generality of global Moran's I index in tracking the dynamic of surface water patterns at a large scale. Large-scale computation of global Moran's I based on images was not a cost-effective manner as it needs to deal with the spatial weight between each pair of spatial locations (Das and Ghosh 2017). The future work should consider such limitation in the use of the proposed framework for large-scale monitoring of water dynamics.

5. Conclusions

Spatial autocorrelation approach was preliminarily tested to quantify the long-term dynamics of surface water patterns in terms of water shrinkage and expansion in a lake-type reservoir during 1985–2018, by computing global Moran's I index based on yearly MNDWI composites. Comparing with discrete landscape indices, although the amplitude of global Moran's I index did not change much during the whole study period, it could successfully assessed the variability of the area, elongation and fragmentation of surface

water in reservoir landscape. The proposed framework might be applied in the areas where the surface water extraction is difficult and water dynamic patterns are complex.

Author contributions

Z.L. led the research, implemented data analysis, reviewed the bibliography and wrote the paper. Y.F. participated in the data collection and data processing. H.G., L.X. and N.D. provided important inputs for this paper. P.G. provided important inputs and reviewed the manuscript. All authors read and approved the final manuscript.

Declaration of interest statement

The authors declare no conflict of interest.

Funding

This research was supported by the National Natural Science Foundation of China (NSFC) (Grant number: 41801336).

References

Cliff, A. D., and J. K. Ord. 1981. *Spatial Processes: Models and Applications*. Pion Limited, London.

Das, M., and S. K. Ghosh. 2017. "Measuring Moran's I in a Cost-Efficient Manner to Describe a Land-Cover Change Pattern in Large-Scale Remote Sensing Imagery." *IEEE Journal of Selected Topics in Applied Earth Observations and Remote Sensing* 10 (6): 2631–2639. doi:10.1109/jstars.2017.2660766.

Drakou, E. G., A. S. Kallimanis, S. P. Sgardelis, and J. D. Pantis. 2008. "Landscape Structure and Habitat Composition in Reservoirs, Lakes, and Rivers." *Lake and Reservoir Management* 24 (3): 244–260. doi:10.1080/07438140809354065.

Du, Y., Y. Zhang, F. Ling, Q. Wang, L. Wenbo, and L. Xiaodong. 2016. "Water Bodies' Mapping from Sentinel-2 Imagery with Modified Normalized Difference Water Index at 10-m Spatial Resolution Produced by Sharpening the SWIR Band." *Remote Sensing* 8 (4): 354. doi:10.3390/rs8040354.

Du, Z., L. Wenbo, D. Zhou, L. Tian, F. Ling, H. Wang, Y. Gui, and B. Sun. 2014. "Analysis of Landsat-8 OLI Imagery for Land Surface Water Mapping." *Remote Sensing Letters* 5 (7): 672–681. doi:10.1080/2150704x.2014.960606.

Evans, I. S., D. T. Robinson, and R. C. Rooney. 2017. "A Methodology for Relating Wetland Configuration to Human Disturbance in Alberta." *Landscape Ecology* 32 (10): 2059–2076. doi:10.1007/s10980-017-0566-z.

Feng, L., H. Chuanmin, X. Chen, X. Cai, L. Tian, and W. Gan. 2012. "Assessment of Inundation Changes of Poyang Lake Using MODIS Observations between 2000 and 2010." *Remote Sensing of Environment* 121: 80–92. doi:10.1016/j.rse.2012.01.014.

Fisher, A., and T. Danaher. 2013. "A Water Index for SPOT5 HRG Satellite Imagery, New South Wales, Australia, Determined by Linear Discriminant Analysis." *Remote Sensing* 5 (11): 5907–5925. doi:10.3390/rs5115907.

Havel, J. E., C. E. Lee, and J. V. Zanden. 2005. "Do Reservoirs Facilitate Invasions into Landscapes?" *Bioscience* 55 (6): 518–525. doi:10.1641/0006-3568(2005)055.

He, G., H. Fang, S. Bai, X. Liu, M. Chen, and J. Bai. 2011. "Application of a Three-dimensional Eutrophication Model for the Beijing Guanting Reservoir, China." *Ecological Modelling* 222 (8): 1491–1501. doi:10.1016/j.ecolmodel.2010.12.006.

Ji, L., P. Gong, J. Wang, J. Shi, and Z. Zhu. 2018. "construction of the 500-m Resolution Daily Global Surface Water Change Database (2001-2016)." *Water Resources Research* 54 (12): 10,270–10,92. doi:10.1029/2018wr023060.

Jiang, P., L. Cheng, L. Manchun, R. Zhao, and Q. Huang. 2014. "Analysis of Landscape Fragmentation Processes and Driving Forces in Wetlands in Arid Areas: A Case Study of the Middle Reaches of the Heihe River, China." *Ecological Indicators* 46: 240–252. doi:10.1016/j.ecolind.2014.06.026.

Li, W., Y. Qin, Y. Sun, H. Huang, F. Ling, L. Tian, and Y. Ding. 2015. "Estimating the Relationship between Dam Water Level and Surface Water Area for the Danjiangkou Reservoir Using Landsat Remote Sensing Images." *Remote Sensing Letters* 7 (2): 121–130. doi:10.1080/2150704x.2015.1117151.

Li, Z., Y. Feng, N. Dessay, E. Delaitre, H. Gurgel, and P. Gong. 2019. "Continuous Monitoring of the Spatio-Temporal Patterns of Surface Water in Response to Land Use and Land Cover Types in a Mediterranean Lagoon Complex." *Remote Sensing* 11 (12): 1425. doi:10.3390/rs11121425.

Li, Z., E. Roux, N. Dessay, R. Girod, A. Stefani, M. Nacher, A. Moiret, and F. Seyler. 2016. "Mapping a Knowledge-Based Malaria Hazard Index Related to Landscape Using Remote Sensing: Application to the Cross-Border Area between French Guiana and Brazil." *Remote Sensing* 8 (4): 319. doi:10.3390/rs8040319.

Liu, R., J. Liu, Z. Zhang, A. Borthwick, and K. Zhang. 2015. "Accidental Water Pollution Risk Analysis of Mine Tailings Ponds in Guanting Reservoir Watershed, Zhangjiakou City, China." *International Journal of Environmental Research and Public Health* 12 (12): 15269–15284. doi:10.3390/ijerph121214983.

Otsu, N. 1979. "A Threshold Selection Method from Gray-Level Histograms." *IEEE Transactions on Systems, Man, and Cybernetics* 9: 62–66. doi:10.1109/TSMC.1979.4310076.

Pflugmacher, D. 2007. "Moderate Resolution Remote Sensing Alternatives: A Review of Landsat-like Sensors and Their Applications." *Journal of Applied Remote Sensing* 1 (1): 012506. doi:10.1117/1.2819342.

Sun, Z., X. Ru, D. Wenjie, W. Lei, and L. Dengsheng. 2019. "High-Resolution Urban Land Mapping in China from Sentinel 1A/2 Imagery Based on Google Earth Engine." *Remote Sensing* 11 (7): 752. doi:10.3390/rs11070752.

Wang, M., D. Longjiang, K. Yinghai, M. Huang, J. Zhang, Y. Zhao, L. Xiaojuan, and H. Gong. 2019. "Impact of Climate Variabilities and Human Activities on Surface Water Extents in Reservoirs of Yongding River Basin, China, from 1985 to 2016 Based on Landsat Observations and Time Series Analysis." *Remote Sensing* 11 (5): 560. doi:10.3390/rs11050560.

Xu, N. 2018. "Detecting Coastline Change with All Available Landsat Data over 1986–2015: A Case Study for the State of Texas, USA." *Atmosphere* 9 (3): 107. doi:10.3390/atmos9030107.

Yang, X., S. Zhao, X. Qin, N. Zhao, and L. Liang. 2017. "Mapping of Urban Surface Water Bodies from Sentinel-2 MSI Imagery at 10 M Resolution via NDWI-Based Image Sharpening." *Remote Sensing* 9 (6): 596. doi:10.3390/rs9060596.

Yihui, W., L. Guihuan, and W. Rui. 2018. "Eco-Compensati on in Guanting Reservoir Watershed Based on Spatiotemporal Variations of Water Yield and Purification Services." *Journal of Resources and Ecology* 9 (4): 416–425. doi:10.5814/j.issn.1674-764x.2018.04.009.

Zhao, R., Y. Chen, H. Zhou, L. Yiqing, Y. Qian, and L. Zhang. 2008. "Assessment of Wetland Fragmentation in the Tarim River Basin, Western China." *Environmental Geology* 57 (2): 455–464. doi:10.1007/s00254-008-1316-y.

Zou, Z., X. Xiao, J. Dong, Y. Qin, R. B. Doughty, M. A. Menarguez, G. Zhang, and J. Wang. 2018. "divergent Trends of Open-surface Water Body Area in the Contiguous United States from 1984 to 2016 ." *PNAS* 115 (15): 3810–3815. doi:10.1073/pnas.1719275115.